

RESEARCH

Open Access



# Electrochemical degradation of methylene blue accompanied with the reduction of CO<sub>2</sub> by using carbon nanotubes grown on carbon fiber electrodes

Nhat Huy Luan, Yu-Ting Yang and Chiung-Fen Chang\*

## Abstract

In this study, the degradation of Methylene Blue (MB) dye accompanied with the reduction of CO<sub>2</sub> was performed in an electrochemical (EC) process by using carbon nanotubes grown on carbon fiber (CNTs/CF<sub>M</sub>) electrodes as the cathode and anode in a two-compartment electrochemical cell. The growth of CNTs on CF<sub>M</sub> via chemical vapor deposition led to the significant improvement in physicochemical properties of CNTs/CF<sub>M</sub> which were beneficial for the EC process. The effects of various operating parameters including supporting electrolytes (KHCO<sub>3</sub> and H<sub>2</sub>SO<sub>4</sub>), initial concentration of MB (5, 10, 15 and 20 mg L<sup>-1</sup>) and applied currents (10, 50 and 100 mA) on the degradation of MB were investigated. The results confirmed the vital influence of applied current and initial concentration of MB while the supporting electrolytes played a minor role in MB degradation. On the contrary, the influence of electrolytes in the performance of CO<sub>2</sub> reduction was more significant on the production and selectivity of generated products. The optimal electrochemical system included 0.1 M KHCO<sub>3</sub> as the electrolyte and an applied current of 50 mA in anodic cell and CO<sub>2</sub> saturated solution in cathodic cell; such a system resulted in the EC degradation efficiency of 72% at the MB initial concentration of 10 mg L<sup>-1</sup> in the anodic cell and production of 4.7 mM cm<sup>-2</sup> CO, 67 mM cm<sup>-2</sup> H<sub>2</sub>, and 11.3 mg L<sup>-1</sup> oxalic acid in the cathodic cell corresponding to the Faradaic efficiencies of 28, 40 and 4%, respectively. The results of reusability test deduced that the stability of CNTs/CF<sub>M</sub> was still satisfactory after 4 runs. The results of this study demonstrated the good applicability of CNTs/CF<sub>M</sub> to be simultaneously used the electrodes for the EC oxidation of dye and the EC reduction of CO<sub>2</sub> to obtain valuable compounds.

**Keywords:** Electrochemical oxidation, Electrochemical reduction of CO<sub>2</sub>, Carbon nanotubes, Methylene blue, Degradation

## 1 Introduction

Rapid increases in the global population over the last few decades and the concomitant surge in human activities have induced great pressures on the environment, especially in terms of water quality. The presence of refractory organic compounds or harmful substances, such as dyes and pigments, in wastewater may cause harm to

the environment. It is estimated that 700 kt of dyes per year are produced for various industries, and used in textiles, food and beverage processing, leather dyeing, plastic and rubber dyeing, and printing processes [1], in which the textile contributes the highest proportion (i.e., up to 54%) of dye effluent [2]. Typically, one ton of textile approximately consumes 21–377 m<sup>3</sup> of water and discharge the huge amount of dye-containing wastewater to the receiving water body, in which 42% of the constituent is refractory for the conventional wastewater

\* Correspondence: [cfchang@thu.edu.tw](mailto:cfchang@thu.edu.tw)

Department of Environmental Science and Engineering, Tunghai University, Taichung 407, Taiwan



© The Author(s). 2022 **Open Access** This article is licensed under a Creative Commons Attribution 4.0 International License, which permits use, sharing, adaptation, distribution and reproduction in any medium or format, as long as you give appropriate credit to the original author(s) and the source, provide a link to the Creative Commons licence, and indicate if changes were made. The images or other third party material in this article are included in the article's Creative Commons licence, unless indicated otherwise in a credit line to the material. If material is not included in the article's Creative Commons licence and your intended use is not permitted by statutory regulation or exceeds the permitted use, you will need to obtain permission directly from the copyright holder. To view a copy of this licence, visit <http://creativecommons.org/licenses/by/4.0/>.

treatment processes [3]. The extensive use of dyes and ineffective treatment processes for dye-containing wastewater have resulted in the detection of dye residues in water bodies and a series of environmental issues, including water eutrophication, low light penetration, dissolved oxygen depletion, and chemical toxicity, all of which exert detrimental impacts to the aquatic ecosystem and humans. Methylene Blue (MB) is a common heterocyclic dye used in many industries. Although numerous efforts to degrade dyes prior to their disposal have been made, conventional wastewater treatment processes are unable to treat MB and other dye compounds sufficiently on account of their complex structures [4]. It is reported that the less color removal efficiency of 67% was obtained via an anaerobic-aerobic biological system [5]. The advanced oxidation processes (AOPs) with ozone, Fenton reagent, and several other approaches show high efficiency for degrading these refractory compounds. Nevertheless, they generally feature some disadvantages, including high cost, waste generation, toxic by-products formation, and elaborate operating procedures [3].

New AOPs based on electrochemical technology have recently been proposed as effective and green solutions to treat refractory organic compounds. Fernandes et al. [6] and Sakalis et al. [7] reported that the efficient degradation of dye by electrochemical (EC) oxidation process, of which the results indicated that over 90% of COD removal and 94% of dye elimination were achieved. These methods are based on the EC generation of reactive oxygen species (ROS), which are powerful oxidizing agents that can mineralize organics to carbon dioxide (CO<sub>2</sub>) [8]. EC oxidation is considered an economical, safe, and green technology for wastewater treatment because it generates ROS on an active electrode surface under low temperatures, consumes small amounts of energy, and produces minimal waste. Therefore, EC oxidation has been applied for the removal of large groups of organic compounds [9].

EC reduction of CO<sub>2</sub> into valuable chemicals is regarded as an innovative approach to reduce greenhouse gas emissions. Various target products may be obtained from the CO<sub>2</sub> reduction reaction (CO<sub>2</sub>RR) depending on the electron transfer mechanism and operating conditions applied. In general, the main products generated during the CO<sub>2</sub>RR are C1 compounds (e.g., carbon monoxide [10], formic acid, and methanol [11]) or C2 compounds (e.g., ethanol [12], acetate, and ethylene [13]). The hydrogen evolution reaction, which is a side reaction of the EC reduction process in aqueous solution, also leads to the generation of hydrogen (H<sub>2</sub>), which, in combination with carbon monoxide (CO), may be used as a gaseous fuel for syngas [14] or feedstock for methanol synthesis via the Fischer–Tropsch process

[15]. Most of these products are high energy-containing products.

Electrode materials are well known to play a significant role in the oxidation/reduction process. Reactive electrodes for oxidation/reduction should possess not only high electrocatalytic activity to degrade organics or to obtain the desired products from the CO<sub>2</sub>RR but also low activity for side reactions, such as the oxygen evolution reaction (OER)/hydrogen evolution reaction (HER) [16]. A considerable number of studies on the development of novel electrodes based on noble metals, metal oxides, dimensionally stable anodes, and boron-doped diamond [15, 16], among others, have been introduced. However, most of the proposed strategies suffer from the drawbacks of high cost, complicated synthesis procedures, and short service lives; some of the electrodes obtained may even release toxic substances to the environment [17].

Carbon-derived materials have attracted great interest from the academic community on account of their inexpensive and abundant resources, physicochemical stability, and wide potential window [18]. However, pristine carbon materials, such as activated carbon and carbon fiber (CF), are seldom employed as reactive electrodes because of their electrochemical inertness, low oxygen evolution potential, and oxidant generation inefficiency [19]. Indeed, these challenges were illustrated in previous reports on the EC oxidation/reduction of Amaranth azo dye using activated CF and the EC oxidation of amoxicillin with CF and carbon graphite [20]. Relatively low decolorization efficiency of 54% and COD removal of 74% were also recorded [21] by using activated CF electrode. The disadvantages of these materials ascribed to the disordered structure of amorphous carbons. Pristine carbon electrodes are also ineffective for EC reduction of CO<sub>2</sub> because CO<sub>2</sub> may not be activated by neutral carbon atoms [19]. Previous reports revealed that the electronic properties of carbon can be significantly improved by converting raw carbon into nanostructured materials [22]. In particular, carbon nanotubes (CNTs) exhibit high electrical conductivity, large surface areas, high chemical stability, and strong efficiency for CO<sub>2</sub> reduction and organics oxidation. The high specific surface area and excellent electronic properties of CNTs provide numerous active sites that could promote electron transfer during the electrochemical reaction. Hydrophobic CNTs are also favorable materials for the adsorption of aromatic pollutants and CO<sub>2</sub> on the surface of electrodes because they can enhance the efficiency of redox reactions.

To the best of our knowledge, although a great number of studies have evaluated the EC oxidation of organics and reduction of CO<sub>2</sub>, reports on the use of CNTs as electrodes in these processes are relatively

scarce. Furthermore, fewer studies discuss about the simultaneous oxidation of organics and reduction of  $\text{CO}_2$  in a two-compartment cell. Thus, in the present work, we investigated the EC oxidation of MB and accompanied with the reduction of  $\text{CO}_2$  in a two-compartment cell by using CNTs grown on carbon fiber (CNTs/ $\text{CF}_M$ ) electrodes. The effects of key operating parameters, such as the electrode materials, initial concentrations of MB, supporting electrolytes and applied currents were also evaluated. Finally, the degradation efficiency of MB, the reduction of  $\text{CO}_2$ , and the generation of  $\text{H}_2$  and other products were monitored.

## 2 Experimental design

### 2.1 Synthesis and characterization of CNTs/ $\text{CF}_M$

The chemical vapor deposition (CVD) method was adopted to grow CNTs on CF. First, pristine CF ( $190 \times 190$  mm, ElectroChem, USA) was coated with titanium (Ti) of 75 nm and nickel (Ni) of 15 nm via E-Gun Evaporation System (ULVAC Technologies, USA); The Ti and Ni coated CF was designated  $\text{CF}_M$ . Next, the  $\text{CF}_M$  was cut into sheets measuring  $30 \times 10$  mm and then placed in the quartz chamber of a CVD reactor (Jyi-Goang, Enterprise Co. Taiwan) to grow the CNTs as follows. The chamber was flushed with  $259 \text{ mL min}^{-1}$  argon (Ar) at a heating rate of  $72.5 \text{ K min}^{-1}$  until the temperature of 1023 K was reached. Next, of  $126 \text{ mL min}^{-1}$  Ar and  $70 \text{ mL min}^{-1}$  ammonia ( $\text{NH}_3$ ) were simultaneously injected into the chamber for 10 min at 1023 K. Then,  $193 \text{ mL min}^{-1}$  Ar,  $32 \text{ mL min}^{-1}$   $\text{NH}_3$ , and  $11 \text{ mL min}^{-1}$  acetylene ( $\text{C}_2\text{H}_2$ ) were used to grow CNTs on the  $\text{CF}_M$  over a period of 25 min at a fixed temperature of 1023 K. Finally, the chamber was naturally cooled to room temperature, and the resultant material (CNTs/ $\text{CF}_M$ ) was collected for further analysis. All flow rates

were controlled by a mass controller (5850E, Brooks). The morphology and graphitization degree of the obtained material were characterized by field emission scanning electron microscopy (FE-SEM, JSM-7800F, JEOL), transmission electron microscopy (TEM, JEM-2100, JEOL), and Raman microscopy (DXR3, Thermo Scientific).

### 2.2 Electrochemical system

The galvanostatic experiments were conducted at a temperature of 298 K in a two-compartment cell separated by a proton exchange membrane (Nafion 212, Dupont). The system was operated in batch mode with a solution volume of 100 mL per cell under magnetic stirring at 300 rpm. The cathodic cell was saturated with high-purity  $\text{CO}_2$  gas prior to the electrochemical experiments, while the anodic cell was filled with MB solution at various initial concentrations. A three-electrode system was used to conduct the degradation experiments; here, the synthesized CNTs/ $\text{CF}_M$  was adopted as the cathode for all experiments;  $\text{CF}$ ,  $\text{CF}_M$ , and CNTs/ $\text{CF}_M$  were investigated as anodes; and Ag/AgCl (saturated with 3.0 M KCl solution) served as the reference electrode. The electrode current was controlled by an electrochemical analyzer (627D, CH Instruments, USA). The CVD and electrochemical systems adopted in this study are shown in Figs. 1 and 2, respectively.

### 2.3 Electrochemical oxidation and reduction

All of the chemicals used in this study were of reagent grade and applied without further purification. Two electrolytes, namely, 0.1 M  $\text{KHCO}_3$  (99%, Alfa Aesar) and 0.1 M  $\text{H}_2\text{SO}_4$  (95–97%, Honeywell) were employed to explore the effect of the supporting electrolyte on the oxidation of MB (reagent grade, Merck) and reduction

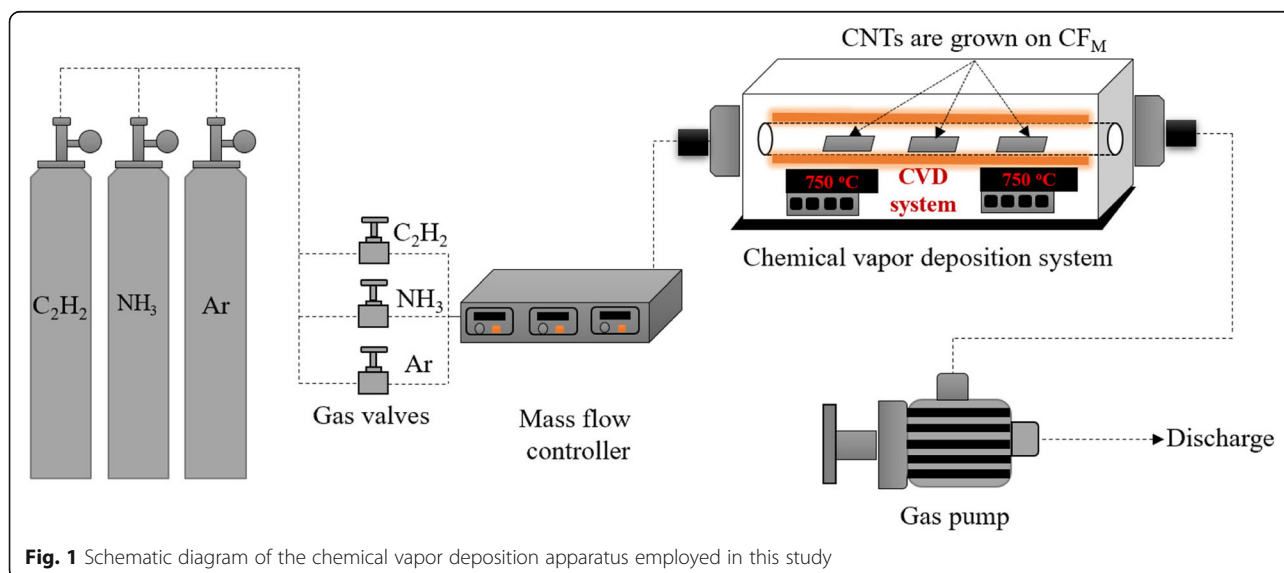


**Fig. 1** Schematic diagram of the chemical vapor deposition apparatus employed in this study

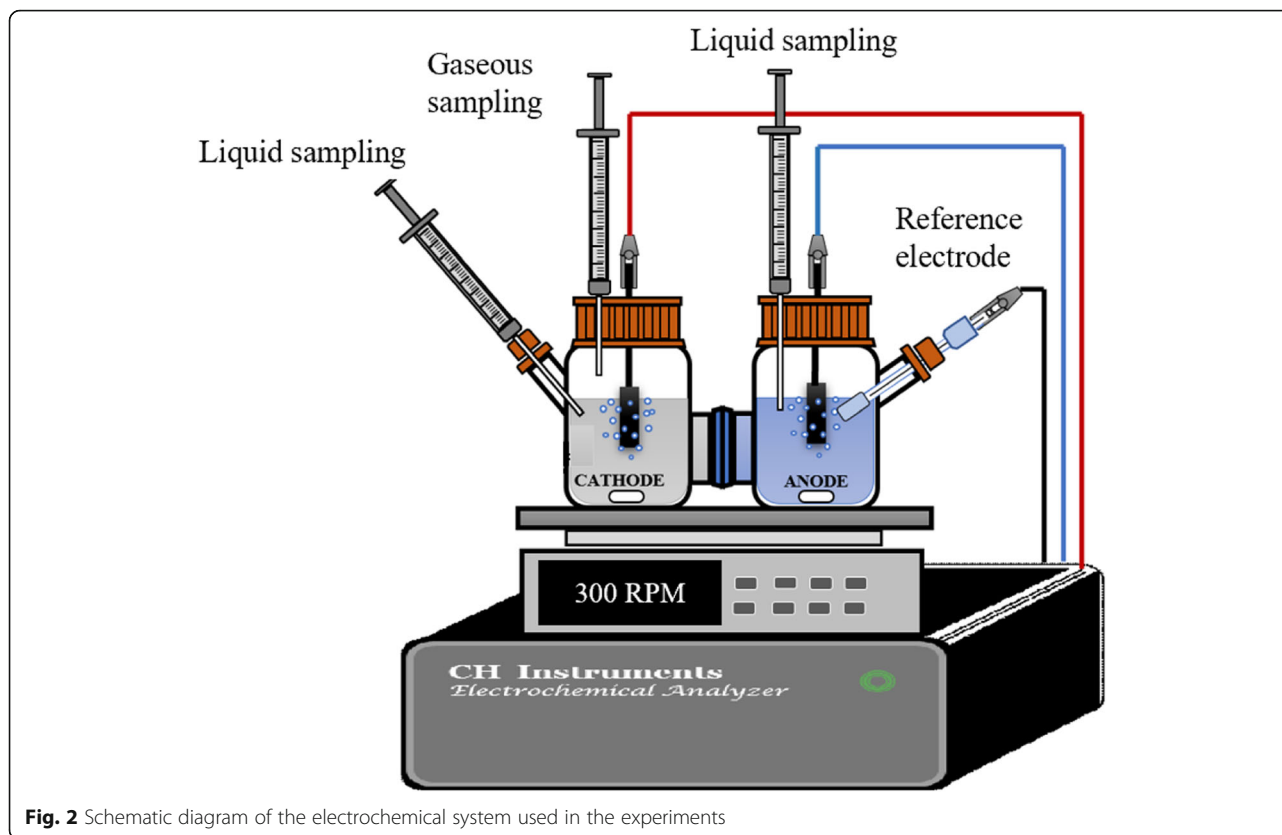


**Fig. 2** Schematic diagram of the electrochemical system used in the experiments

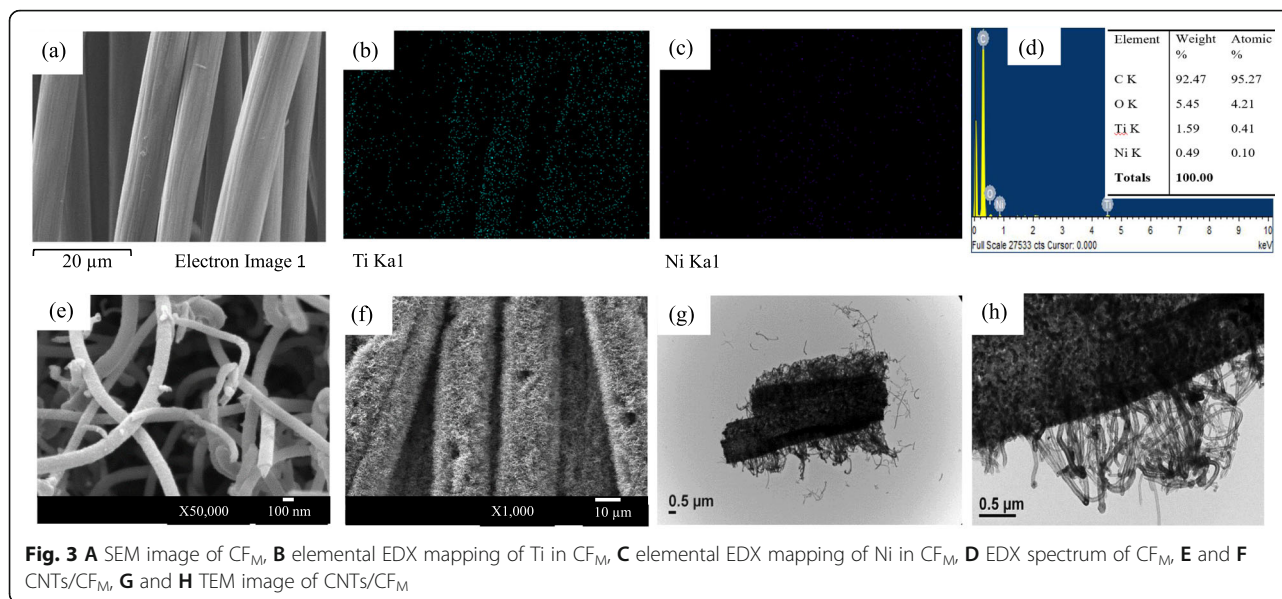
of CO<sub>2</sub> (99.9%, Nini Air Co., Taiwan). CO<sub>2</sub> saturation of the cathodic cell was conducted by purging with high-purity CO<sub>2</sub> gas at a rate of 50 mL min<sup>-1</sup> for 30 min prior to initiation of the EC reactions. The experiments were conducted under various electrolytes and applied currents (10, 50, and 100 mA), and samples were withdrawn at designated time intervals. The concentrations of CH<sub>4</sub>, CO, and H<sub>2</sub> in gaseous samples were determined by a gas chromatograph equipped with a thermal conductivity detector (GC/TCD; G3440B, Agilent Technologies, Palo Alto, CA, USA), and the concentration of oxalic acid in liquid samples was assessed by a high-performance liquid chromatograph (HPLC; LC-20AT, Shimadzu, Japan) with a UV/Vis detector (SPD-20, Shimadzu). The columns used for the GC/TCD and HPLC/UV analyses were a Mol Sieve 5A Plot column and an Acclaim™ Organic Acid column, respectively. The carrier gas for H<sub>2</sub> and CO was nitrogen, and the carrier gas for CH<sub>4</sub> was helium (99.9%). The gases were purified by a renewable gas purification system (G3440-60003, Agilent Technologies) prior to their injection into the main column. Liquid samples were passed through a 0.45 μm filter prior to analysis. The MB concentration in the EC system was measured at various time intervals by a UV-Vis spectrophotometer (S-3150, Scinco) with a photodiode array detector at a wavelength of 655 nm. All experiments were repeated twice to ensure their

reproducibility for quality assurance and control. The UV-Vis absorption spectrum of MB and its calibration curve are illustrated in Fig. S1.

### 3 Results and discussion

#### 3.1 Characteristics of the obtained electrodes

The morphologies of CF<sub>M</sub> and CNTs/CF<sub>M</sub> are illustrated in Fig. 3. Figure 3a indicates that the average diameter of carbon fibers is around 7.7 μm. Minimal differences in appearance were noted between CF and CF<sub>M</sub> (as shown in Fig. S2a and S2b) because the Ti and Ni nanoparticles attached to the former are relatively small. SEM-EDX mapping of CF<sub>M</sub> was conducted to confirm the presence of metallic nanoparticles, as shown in Figs. 3b–d. The results revealed that Ti and Ni nanoparticles were well distributed on the surface of CF and respectively accounted for approximately 1.6 and 0.5 wt%, respectively. Such a tiny amount of Ti and Ni nanoparticles facilitated the growth of CNTs over the CF<sub>M</sub> layer during the CVD process. Figure 3e indicates that CNTs were grown randomly and thickly on the CF<sub>M</sub> surface. The diameters of the grown CNTs are less than 100 nm. The arrays of dense CNTs almost covered the whole external area of CF<sub>M</sub> leading to the significant increase of specific area of the electrode, as illustrated in Fig. 3f. To further characterize the micro-morphology of CNTs/CF<sub>M</sub>, TEM analysis was also carried out and illustrated in Fig. 3g



and h. The images show the rope-like shapes of CNTs with the hollow internal structure which create the ultrahigh surface-to-volume ratio of the CNTs/ $CF_M$ . The nanoscale structures of the CNTs could provide abundant active sites, improve the adsorption of target compounds on the electrode surface, and enhance the electronic conductivity of the electrode, which facilitates the rapid transport of electrons through the electrolyte/electrode interface during electrolysis.

Raman spectroscopy was employed to characterize the graphitic structure of the carbon materials and investigate the quality of the CNTs grown on  $CF_M$  further [23]. The ratio of the peak intensities of the D ( $I_D$ ) and G ( $I_G$ ) bands is a good indicator of the quality of graphitization [24]. Figure 4 illustrates the Raman spectra of  $CF_M$  and CNTs/ $CF_M$ , both of which are graphite-like materials. The spectra of both samples revealed the peaks of the D and G bands at wavenumbers of 1310 and 1580  $cm^{-1}$ , respectively, which were also represented the  $sp^3$  and  $sp^2$  bonds, respectively. The greater value of  $I_D$  reflects the dominance of the amorphous structure of carbon over the graphite structure in both samples in this study. The  $I_D/I_G$  ratios of  $CF_M$  and CNTs/ $CF_M$  were 1.68 and 1.45, respectively, which confirms the lower ratio of  $I_D/I_G$  of CNTs/ $CF_M$  compared with that of  $CF_M$  and demonstrates the enhanced graphitization of CNTs/ $CF_M$  due to the growth of CNTs on  $CF_M$ . Furthermore, the hybridization of  $sp^2/sp^3$  provides the greater physicochemical strength for the material due to the strong bond of  $sp^2$ . The weight of  $CF_M$  before and after CNTs growth was determined to investigate the weight percentage of CNTs in the composite. The weight of  $CF_M$  increased by 0.086 wt% after the

growth of CNTs. Although the disordered carbon structure dominates  $CF_M$  and CNTs/ $CF_M$ , CNTs growth on the surface of the former clearly promotes the graphitization and purity of the latter. These results are in agreement with the FE-SEM analysis.

### 3.2 Electrochemical degradation of MB

#### 3.2.1 The effect of various electrodes on the electrochemical degradation of MB

The presence of metallic nanoparticles on the CNTs could provide catalytic support to  $CF_M$ . Although the metallic nanoparticles observed on  $CF_M$  comprised a relatively low weight percentage of the total material, the former may still function as electrocatalysts in the EC process. Therefore, raw CF,  $CF_M$ , and CNTs/ $CF_M$  were used as anodes to investigate the effects of Ti and Ni on the EC degradation of MB, as shown in Fig. 5. The EC degradation efficiencies of MB with raw CF,  $CF_M$  and CNTs/ $CF_M$  in solution after 3 h were approximately 25, 29, and 66%, respectively. The decay of MB could be attributed to direct electron transfer (i.e., direct oxidation) on the surface of the anode under an electric field. The comparison of the degradation efficiencies of MB with CF and  $CF_M$  indicated that the metallic nanoparticles did not exert a remarkable effect on the electronic properties of raw CF, and the degradation efficiency of MB increased by only 4% after the nanoparticles were coated on the CF. By contrast, CNTs/ $CF_M$  showed a great increase in MB degradation efficiency, thus confirming the important role of CNTs in EC degradation. This finding may be attributed to the large specific area and spacious nano-channels on the surface of the CNTs, which promote the adsorption, and mass transfer of MB onto the electrode surface. The excellent

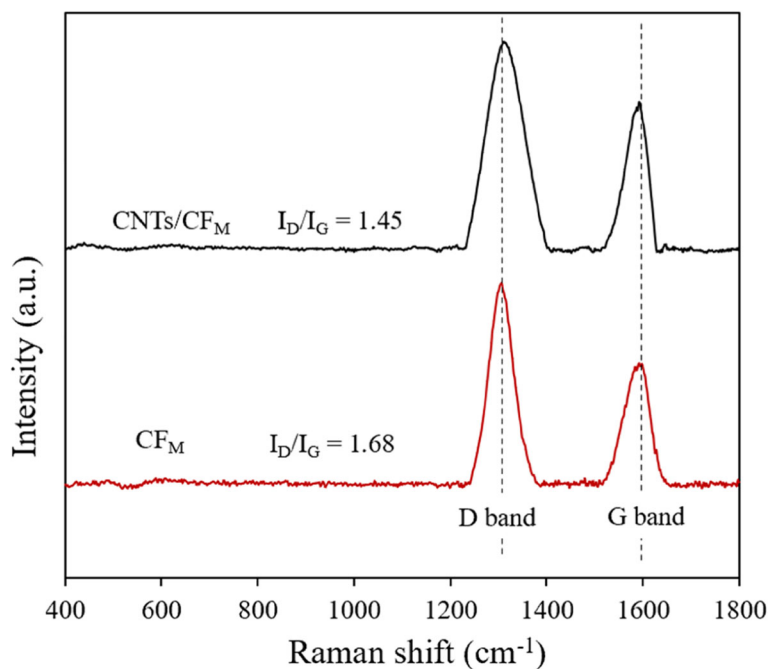


**Fig. 4** Raman spectra of  $CF_M$  and  $CNTs/CF_M$

electrical conductivity of the highly graphitized structure of CNTs could also enhance the exchange and transport of electrons. These synergistic effects led to significant increases in the oxidation performance of the resultant electrode for MB degradation.

**3.2.2 The role of applied current on the electrochemical degradation of MB**

The mechanism of the EC oxidation of MB is illustrated in Eqs. (1) and (2) and Fig. 6. MB degradation typically occurs on the surface of anodic  $CNTs/CF_M$  via the

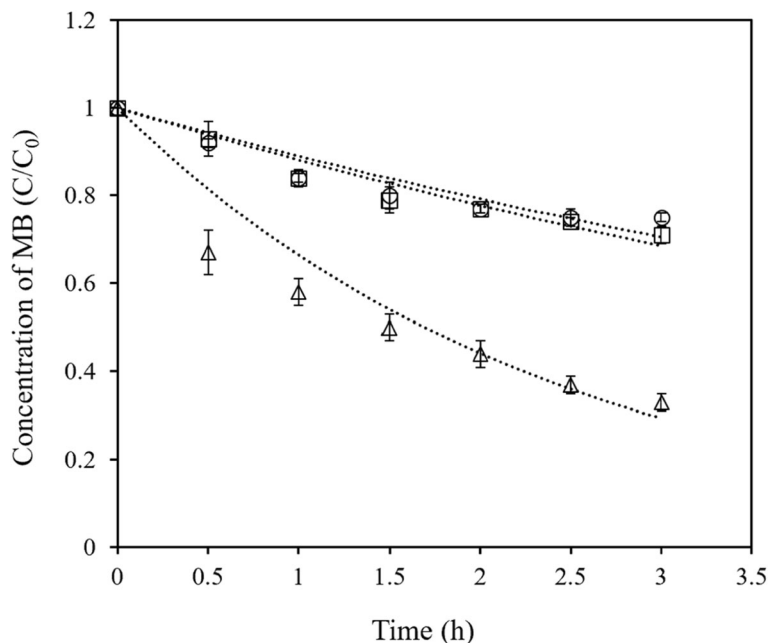
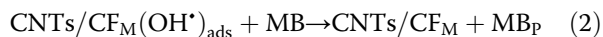
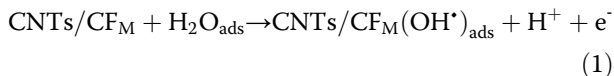


**Fig. 5** Electrochemical degradation efficiencies of MB with various anodic electrode materials in solution under an applied current of 50 mA, electrolyte of 0.1 M  $H_2SO_4$ , initial MB concentration of  $10\text{ mg L}^{-1}$ , initial pH value of the solution of 1.83 and cathode of  $CNTs/CF_M$ .  $\Delta$ :  $CNTs/CF_M$ ;  $\square$ :  $CF_M$ ;  $\circ$ :  $CF$

generation of hydroxyl radicals (OH•). The efficiency of this process may strongly depend on applied current and supporting electrolytes. Thus, the effects of these parameters were investigated further, and the pseudo-first-order kinetic model was employed to define the degradation kinetics of MB under various conditions, as shown in Eqs. (3) and (4).



where MB<sub>P</sub> represents the oxidation by-products of MB.

$$\frac{-d[\text{C}]}{dt} = k_{\text{obs}} \times [\text{C}] \quad (3)$$

$$\ln \frac{[\text{MB}]_0}{[\text{MB}]} = k_{\text{obs}} \times t, \text{ with } t = 0, [\text{C}] = [\text{MB}]_0; t = t, [\text{C}] = [\text{MB}] \quad (4)$$

where [C] is the concentration of the target compound; t is the reaction time, h; and k<sub>obs</sub> is the rate constant, h<sup>-1</sup>.

The effects of the applied current and electrolyte on the EC degradation efficiency of MB were investigated, as shown in Fig. 7. The results revealed that the applied current plays a key role in the degradation efficiency of MB. An increase in the applied current obviously resulted in improvements in oxidation efficiency with both supporting electrolytes. Specifically, the MB degradation efficiency of electrochemical systems with KHCO<sub>3</sub> and

H<sub>2</sub>SO<sub>4</sub> as electrolytes increased from 56 to 72% and from 66 to 73%, respectively, when the applied current was raised from 10 mA to 50 mA. Increases in the applied current may help enhance the EC generation of OH•, resulting in improved MB degradation efficiency. This finding agrees with the results of previous studies [25] in which the degradation efficiency increased with increasing applied current when a graphite electrode and a CNTs-modified activated carbon electrode were used for the removal of phenol and Methyl Orange, respectively. However, when the current was increased to 100 mA, the degradation efficiency of the electrochemical system decreased to values between those obtained at 10 and 50 mA in KHCO<sub>3</sub> and less than that obtained of 10 mA in H<sub>2</sub>SO<sub>4</sub>. This behavior may be due to a higher current increasing the occurrence of the OER, which leads to a decrease in the current efficiency for the desired reactions [26]. The adsorptive ability and electrocatalytic activity of the electrodes could also be influenced by the by-products generated from decomposition reactions and gases generated from the OER under high applied currents because these substances restrict mass transport [27]. The rapid and massive formation of O<sub>2</sub> from the OER not only reduces the diffusion of MB toward the electrode surface via competitive adsorption but also increases the internal pressure within the CNTs/CF<sub>M</sub> structure. The extensive generation of O<sub>2</sub> and ROS may detach CNTs from the CF<sub>M</sub> substrate and reduce the activity and stability of the electrode. Thus, the greater likelihood of the OER, by-products arising

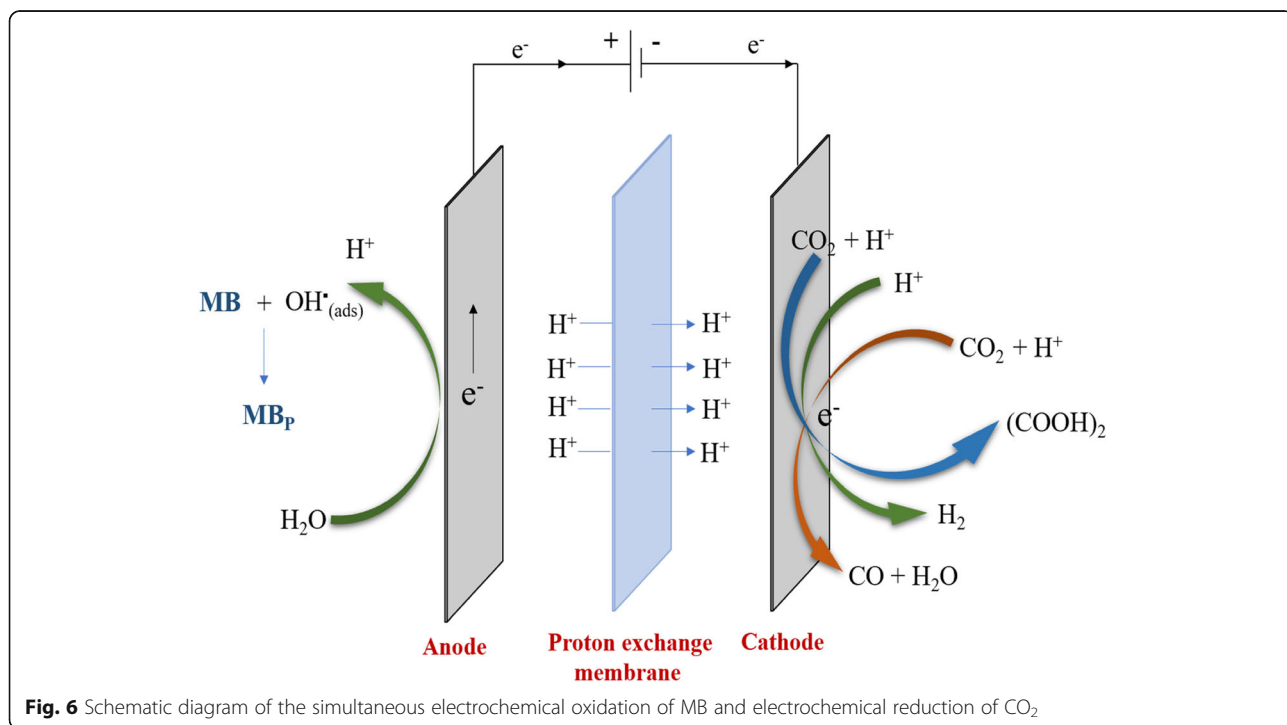
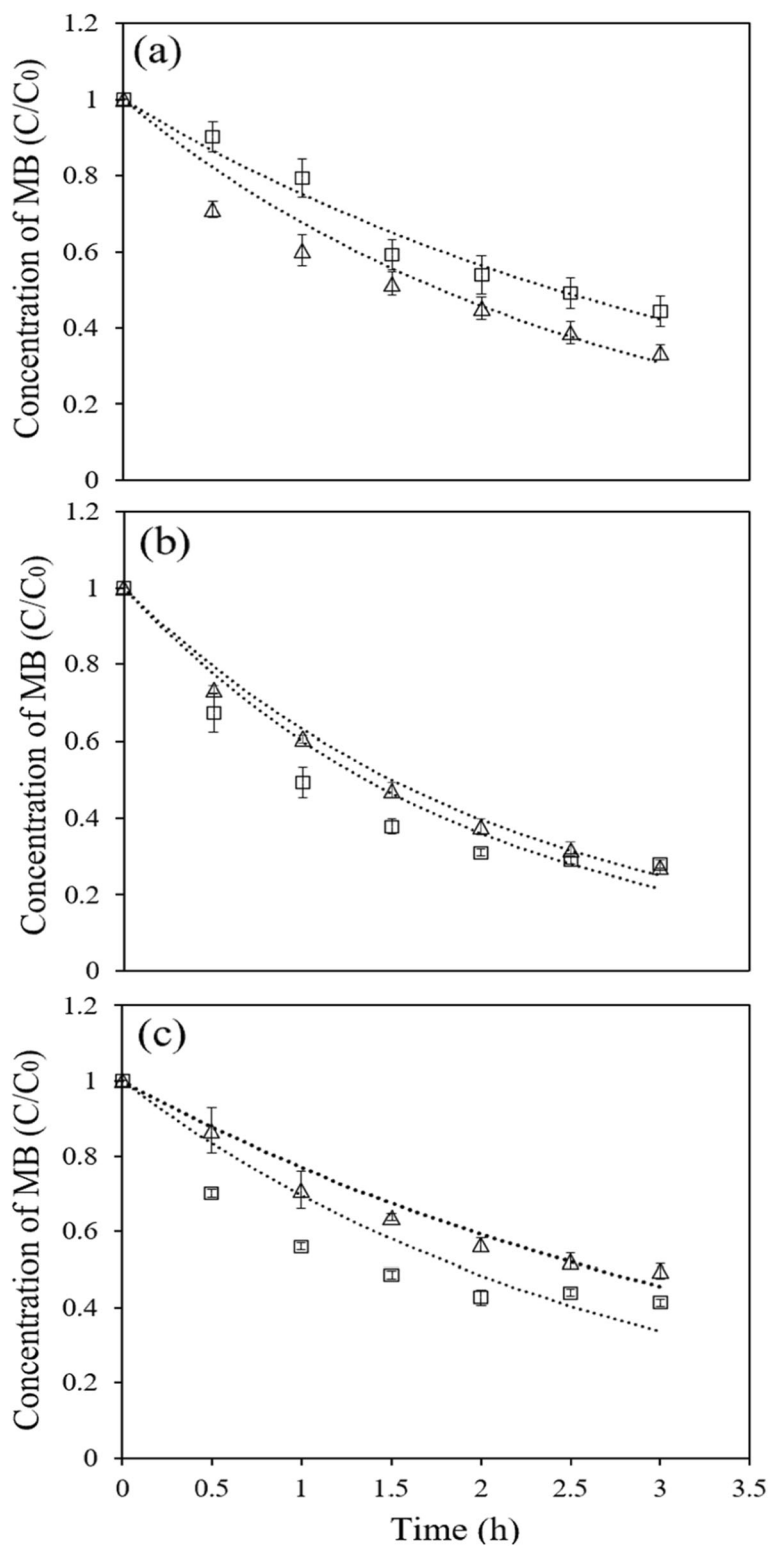


Fig. 6 Schematic diagram of the simultaneous electrochemical oxidation of MB and electrochemical reduction of CO<sub>2</sub>



**Fig. 7** Electrochemical degradation efficiency of MB in solution by using CNTs/CF<sub>M</sub> as both cathode and anode under various electrolytes and applied currents of **A** 10, **B** 50, and **C** 100 mA. □: 0.1 M KHCO<sub>3</sub>; Δ: 0.1 M H<sub>2</sub>SO<sub>4</sub>. Initial MB concentration of 10 mg L<sup>-1</sup>, initial pH value of the solution of 8.19 and 1.83 for 0.1 M KHCO<sub>3</sub> and 0.1 M H<sub>2</sub>SO<sub>4</sub>, respectively

from decomposition reactions and deterioration of the electrode quality render an applied current of 100 mA unfavorable for the EC degradation of MB in solution. The same phenomenon was reported in a previous study [28], which reported that the surface of the electrode is blocked by the coverage of insoluble polymeric products that are relatively slowly oxidized or desorbed when electrolysis with a glassy carbon electrode is conducted at high current densities. Comparison of the effect of  $\text{KHCO}_3$  and  $\text{H}_2\text{SO}_4$  on the MB degradation efficiency revealed that MB is degraded more effectively at low applied currents when  $\text{H}_2\text{SO}_4$  is used as an electrolyte than when  $\text{KHCO}_3$  is employed. Maximum degradation efficiencies of 72 and 73% were respectively obtained under an applied current of 50 mA in EC systems containing  $\text{KHCO}_3$  and  $\text{H}_2\text{SO}_4$  as electrolytes. The pH of the electrolyte is another important parameter that may influence the performance of an electrochemical system. Many reports have proposed that the oxidation process is promoted in acidic electrolytes [29]. The presence of  $\text{H}_2\text{SO}_4$  may inhibit the OER reaction, which typically causes detrimental effects on the generation of ROS via the consumption of  $\text{OH}\cdot$  radicals. Therefore, more  $\text{OH}\cdot$  radicals are generated on the surface of the electrode to facilitate the degradation reaction in acidic conditions than in basic or neutral conditions. This result is in agreement with an earlier report [30].

The experimental data were collected over a reaction time of 3 h to calculate the corresponding rate constants, as illustrated in Table 1. Comparison of the degradation efficiencies of MB obtained in  $\text{KHCO}_3$  and  $\text{H}_2\text{SO}_4$  indicated that the use of the latter as a supporting electrolyte could achieve higher degradation efficiencies under applied currents of 10 and 50 mA. This result indicates that MB oxidation is favorable in acidic medium. However, among the conditions surveyed in this study, the highest  $k_{\text{obs}}$  ( $0.51 \text{ h}^{-1}$ ) were obtained in the system in which 0.1 M  $\text{KHCO}_3$  as the electrolyte and 50 mA as the applied current was employed.

### 3.2.3 Effect of initial concentration of MB on the efficiency of electrochemical degradation

The effect of the initial concentrations of MB on EC degradation efficiency during the EC process was conducted to simulate the treatment of various concentration of dye-containing wastewaters. The investigation of EC degradation of MB at initial concentrations of 5, 10, 15 and  $20 \text{ mg L}^{-1}$  were examined, as shown in Fig. 8. It can be clearly observed that the higher initial concentration, the lower EC degradation efficiency. At the low concentration of  $5 \text{ mg L}^{-1}$ , the degradation of MB reached to the removal efficiency of 100% after 3-h reaction time. However, the further increase of initial concentration of MB, the degradation efficiencies of MB dropped to approximate 75, 54, and 32% for 10, 15 and  $20 \text{ mg L}^{-1}$ , respectively. This phenomenon can be attributed to the competition of more MB molecules in solution for the fixed amount of ROS generated under the same conditions. Furthermore, the EC degradation of MB also led to the generation of numerous byproducts, which may compete with their pristine MB so as to reduce the degradation efficiency of the parent compound of MB. In addition, it is possible that the adsorption of intermediates on the microstructure of  $\text{CNTs}/\text{CF}_M$  may not only hinder the generation of  $\text{OH}\cdot$  radicals but also reduce the effectiveness of the mass transfer process at high MB concentrations. Consequently, the reduction of the reactivity of electrode and the degradation efficiency is expected in the high MB concentration system.

### 3.2.4 Stability test of $\text{CNTs}/\text{CF}_M$ electrode

The stability and reusability of the electrode in EC process are critical for the practical applicability and feasibility. Thus, the stability test of  $\text{CNTs}/\text{CF}_M$  electrode was carried out toward the degradation of MB for 4 runs under optimum operating conditions. After each run, the electrode was rinsed with DI water, dried in an oven at the temperature of  $65^\circ\text{C}$  in 15 min and then ready for use. Figure 9 shows the degradation efficiency of MB by the anode of  $\text{CNTs}/\text{CF}_M$  for 4-run EC

**Table 1** Rate constants of the pseudo-first-order equation obtained under various electrochemical oxidation conditions

Applied Current, mA	Degradation efficiency, %	$k_{\text{obs}}$ , $\text{h}^{-1}$	Correlation coefficient ( $r^2$ )
Electrolyte of 0.1 M $\text{KHCO}_3$ (for both cathodic and anodic cells), initial pH of 8.19			
10	56	0.29	0.9907
50	72	0.51	0.9688
100	59	0.36	0.9455
Electrolyte of 0.1 M $\text{H}_2\text{SO}_4$ (for both cathodic and anodic cells), initial pH of 1.83			
10	66	0.26	0.9876
50	73	0.46	0.9960
100	50	0.39	0.9866

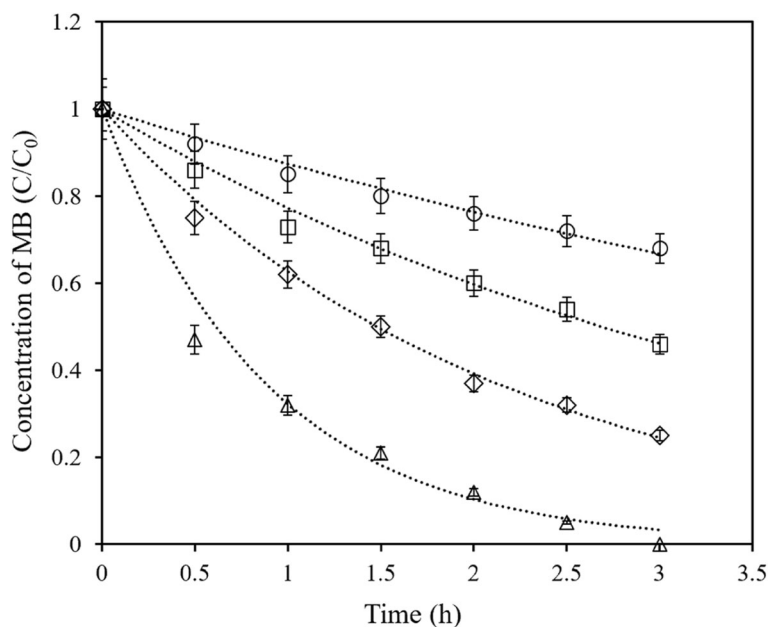


**Fig. 8** Effect of initial concentration of MB on the efficiency of electrochemical degradation by using CNTs/CF<sub>M</sub> as both cathode and anode under an applied current of 50 mA and electrolyte of 0.1 M H<sub>2</sub>SO<sub>4</sub> (initial pH value of 1.83). Initial MB concentration of Δ: 5 mg L<sup>-1</sup>; ◇: 10 mg L<sup>-1</sup>; □: 15 mg L<sup>-1</sup> and ○: 20 mg L<sup>-1</sup>

oxidations. It can be observed that the oxidation performance of electrode showed negligible change in the first two runs. The third and fourth runs resulted in the slight reduction of efficiency, in which the degradation efficiencies were 68 and 64%, respectively. This result

confirmed the good stability of CNTs/CF<sub>M</sub> in EC process in the experimental range. The loss of partial activity of electrode can be attributed to the adsorption of degradation byproducts on the nanostructure of electrode, which gradually reduced the mass transfer

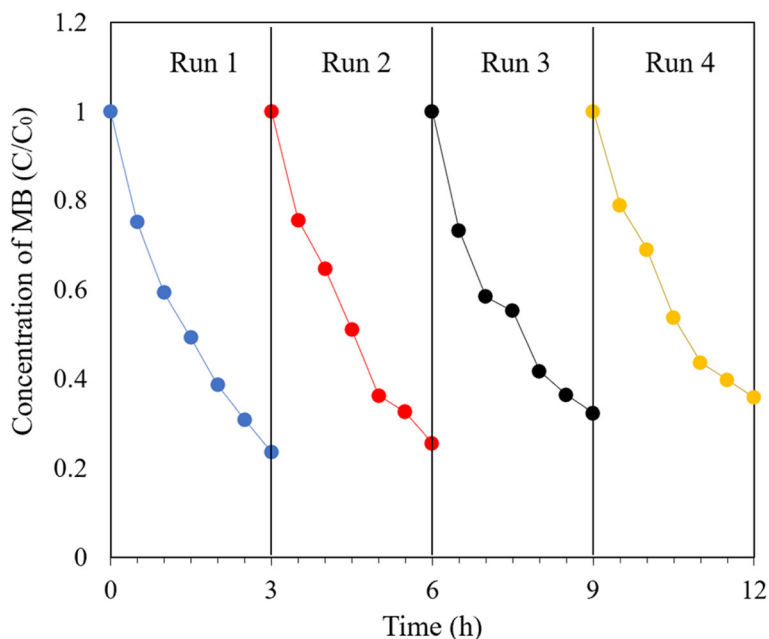


**Fig. 9** Stability test of CNTs/CF<sub>M</sub> electrode via the repeating experiment of electrochemical degradation of MB by using CNTs/CF<sub>M</sub> as both cathode and anode under an applied current of 50 mA and electrolyte of 0.1 M H<sub>2</sub>SO<sub>4</sub> (initial pH value of 1.83). Initial MB concentration of 10 mg L<sup>-1</sup>

of MB to CNTs surface and hinder the generation of ROS. To overcome the disadvantage resulted from byproducts, a thermal treatment of electrode was probably needed [31].

### 3.3 CO<sub>2</sub> reduction and production of by-products

As the EC oxidation of MB in anodic cell, simultaneously, the CO<sub>2</sub>RR and generation of by-products in the cathodic cell were investigated under an applied current of 50 mA. The CO and H<sub>2</sub> obtained from the reduction of CO<sub>2</sub> and electrolysis of H<sub>2</sub>O were determined, as shown in Fig. 10a, b, and Table 2. In general, the efficiency of CO<sub>2</sub>RR is typically related to the concentration of CO<sub>2</sub>, proton (H<sup>+</sup>), and their adsorption on electrode surface. The high conductivity of graphitic structure of CNTs on CNTs/CF<sub>M</sub> promotes the transfer of electrons and the reduction of H<sup>+</sup>. As can be seen in Fig. 10a, the formation of CO increased in cathodic cells containing 0.1 M KHCO<sub>3</sub> and 0.1 M H<sub>2</sub>SO<sub>4</sub> as electrolytes over the process of EC reduction. Moreover, the KHCO<sub>3</sub> system performed better than the H<sub>2</sub>SO<sub>4</sub> system, which indicates that KHCO<sub>3</sub> as an electrolyte is more favorable for CO generation than H<sub>2</sub>SO<sub>4</sub>. The nature of the electrolyte may alter the electrochemical properties of the electrode surface and induce a shift in the onset potential for the CO<sub>2</sub>RR. This finding may be attributed to the adsorption of HCO<sub>3</sub><sup>-</sup> on CNTs/CF<sub>M</sub>, which promotes the formation of CO, and is in agreement with the findings of Verma et al. [32]. On the other hand, the HER typically occurs on the cathode surface in the presence of a high concentration of H<sup>+</sup> and could compete with the CO<sub>2</sub>RR. KHCO<sub>3</sub> may play the role of confining OH<sup>-</sup> and establishing alkaline gradient surrounding electrode surface and then to reduce the availability of H<sup>+</sup> and increase the local concentration of CO<sub>2</sub>. Therefore, the active sites of the electrode for the conversion of CO<sub>2</sub> to CO was remained and the efficiency of HER was reduced. The yield of CO after 3-h reaction time in EC systems containing H<sub>2</sub>SO<sub>4</sub> and KHCO<sub>3</sub> as electrolytes were 3.4 and 4.7 mM cm<sup>-2</sup> corresponding to the faradaic efficiencies of 21 and 28%, respectively; these values are much greater than those obtained from a Cu cathodic electrode (15 μM cm<sup>-2</sup>) and Cu-coated Cu nanoparticles (21 μM cm<sup>-2</sup>) under an applied potential of -0.99 V [25]. The faradaic efficiencies of CO obtained from CNTs/CF<sub>M</sub> in this study are also higher than that (i.e., 3.5%) obtained from a CNTs coated carbon paper electrode [33]. This result may be attributed to the large active area of CNTs on CNTs/CF<sub>M</sub> as compared with the bulk electrode, which led to significant enhancements in CO production. Furthermore, the cations of electrolytes have been demonstrated to possess important effects on the nature and amount of products generated from different electrodes [34, 35]. The bigger size of cation

seems to be easily adsorbed on the cathode surface, which subsequently induces the change in electronic properties of electrode [36]. Due to the higher atomic radius of K<sup>+</sup> (1.33 Å) as compared with H<sup>+</sup> (0.53 Å) dissociated from H<sub>2</sub>SO<sub>4</sub>, the lower outer Helmholtz plane (OHP) potential of CNTs/CF<sub>M</sub> was achieved, and then contributed to the improvement of faradaic efficiency for CO generation.

Figure 10b illustrates the amount of H<sub>2</sub> generated by the use of different electrolytes. H<sub>2</sub> evolution increased with increasing reaction time under both supporting electrolytes, although KHCO<sub>3</sub> could achieve more extensive H<sub>2</sub> generation than H<sub>2</sub>SO<sub>4</sub> under identical conditions. The maximum H<sub>2</sub> production obtained in H<sub>2</sub>SO<sub>4</sub> and KHCO<sub>3</sub> systems were 60 and 67 mM cm<sup>-2</sup>, respectively, which correspond to 37 and 40% of faradaic efficiencies; these values are 16- and 18-fold greater in comparison with the H<sub>2</sub> production rate achieved by a Pt/TiO<sub>2</sub>/CdS/CdSe/PEDOT electrode fabricated for photocatalytic hydrogen production [37]. The high production of H<sub>2</sub> can be attributed to the limit transportation of CO<sub>2</sub> and lower reduction potential, despite the high concentration of CO<sub>2</sub> in the solution. CO<sub>2</sub> is typically adsorbed on the external surface of electrodes while H<sup>+</sup> has greater mobility to access more active sites on the internal surface; as the result, more electrons were consumed by HER so as to increase the production of H<sub>2</sub>. The results are consistent with a previous report [33].

The organic products investigated in this study included formic acid, oxalic acid, methanol, and ethanol; of these, only oxalic acid was found in the samples. The generation of oxalic acid is illustrated in Fig. 10c. This by-product was generated and increased with the reaction time in systems containing H<sub>2</sub>SO<sub>4</sub> and KHCO<sub>3</sub> as supporting electrolytes. When KHCO<sub>3</sub> was adopted as the supporting electrolyte, the production of oxalic acid dramatically increased with the reaction time and peaked at 11.3 mg L<sup>-1</sup> after 3 h; this production rate is approximately two times greater than that obtained when H<sub>2</sub>SO<sub>4</sub> was used as the electrolyte. Moreover, the oxalic acid production rate obtained in this work was 53-fold greater than that obtained in the photocatalytic reduction of CO<sub>2</sub> in water by using TiO<sub>2</sub> nano particles as a catalyst [38]. As mentioned earlier, the cation of the electrolyte could influence the production yield and selectivity of the CO<sub>2</sub>RR via the alternative the OHP potential of electrode. The hydrolysis of water molecules could also result in the formation of a hydration shell around K<sup>+</sup> in the vicinity of the electrocatalytic surface, which facilitates the interaction of adsorbed intermediates on the CNTs surface, where K<sup>+</sup> acts as a catalytic promotor for hydrocarbons. In contrast to the results obtained in this study, oxalic acid was not detected by Kaneco et al. [39], who conducted the EC reduction of CO<sub>2</sub> in KOH-methanol electrolyte with an Ag cathode. Our results also differ considerably from a previous report [40] in which formic acid was obtained as the major liquid

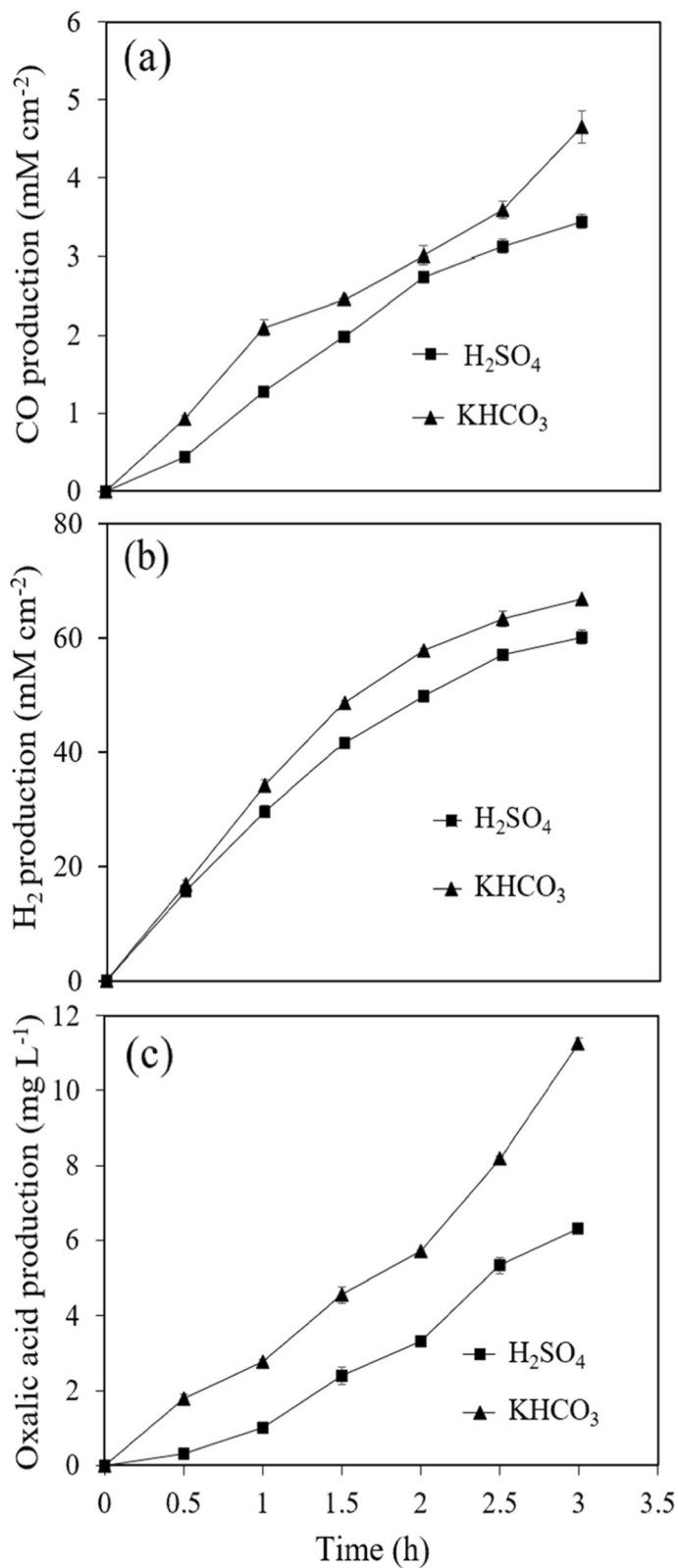


**Fig. 10** Electrochemical generation of **A** CO **B** H<sub>2</sub> and **C** oxalic acid by using CNTs/CF<sub>M</sub> as both cathode and anode under an applied current of 50 mA in various electrolytes. Initial pH values of the solutions are 1.86 and 8.22 for 0.1 M H<sub>2</sub>SO<sub>4</sub> and 0.1 M KHCO<sub>3</sub>, respectively

**Table 2** Faradaic efficiencies of various products obtained after 3 h of CO<sub>2</sub>RR

Electrolyte	CO, % (A)	H <sub>2</sub> , % (B)	Oxalic acid, % (C)	Sum, % (A + B + C)
0.1 M H <sub>2</sub> SO <sub>4</sub> (initial pH of 1.86)	21	37	2	60
0.1 M KHCO <sub>3</sub> (initial pH of 8.22)	28	40	4	72

product following CO<sub>2</sub> reduction by using a metal electrode in KHCO<sub>3</sub> electrolyte. Therefore, the selectivity of by-products in the CO<sub>2</sub> reduction process is not only influenced by the electrode material but also the electrolyte properties. Considering the Faradaic efficiencies for CO<sub>2</sub>RR obtained in this study, KHCO<sub>3</sub> possesses not only better ability to convert CO<sub>2</sub> to CO and oxalic acid but also exhibits greater production of HER as compared with H<sub>2</sub>SO<sub>4</sub>, in which the total faradaic efficiencies were recorded at 72 and 60%, respectively.

#### 4 Conclusions

In the present study, the CNTs/CF<sub>M</sub> electrode has been successfully synthesized by CVD method. The simultaneous EC oxidation of MB and the reduction of CO<sub>2</sub> using CNTs/CF<sub>M</sub> in a two-compartment cell have been studied. The importance of process parameters such as electrode materials, initial concentration of MB, applied current and the supporting electrolytes on the degradation of MB was also analyzed. The results confirm the superior physicochemical property of CNTs/CF<sub>M</sub> due to the growth of CNTs. Applied current is demonstrated as one of the most important factors due to its direct effect on the generation of ROS as well as adsorptive properties and the stability of the electrode. The favorable applied current in this study is in the range of 10–50 mA; a higher current of 100 mA can result in the deterioration of the electrode. The maximum MB degradation efficiency of 100% can be achieved at an initial concentration of 5 mg L<sup>-1</sup> under an applied current of 50 mA. The degradation efficiency is inhibited due to the excessive MB per reactive species and the competition of generated by-products. The supporting electrolyte exhibits the minor effect on the EC oxidation performance. The stability test of CNTs/CF<sub>M</sub> confirms the good reusability of the electrode, and the decay of degradation performance is approximate 10% after the fourth run.

With respect to EC reduction of CO<sub>2</sub>, the electrode of CNTs/CF<sub>M</sub> exhibits good catalytic properties for the conversion of CO<sub>2</sub> into CO, oxalic acid and the production of H<sub>2</sub>. The high activity of CNTs/CF<sub>M</sub> for CO<sub>2</sub>RR is attributed to the great specific area of CNTs which creates the remarkable active sites for reduction reaction. The increase of graphitic structure over amorphous of electrode provides the high electrical conductivity so as to the transfer of electron is significantly enhanced. Compared with the influence of electrolyte sort on EC oxidation, the effect of electrolytes on CO<sub>2</sub>RR is

relatively significant. The highest Faradaic efficiency of 72% was obtained for KHCO<sub>3</sub> electrolyte at such a low applied current of 50 mA, corresponding to the faradaic efficiency of CO (28%), H<sub>2</sub> (40%) and oxalic acid (4%). The results confirm coupling CO<sub>2</sub>RR with the EC oxidation of MB dye not only solves the pollution problem and reduces the CO<sub>2</sub> emission but also produces valuable products.

#### 5 Supplementary Information

The online version contains supplementary material available at <https://doi.org/10.1186/s42834-022-00122-1>.

**Additional file 1: Figure S1.** (a) The full UV-Vis absorption spectra of MB and (b) the calibration curve of MB. **Figure S2.** The FE-SEM images of (a) CF, (b) CF<sub>M</sub> and (c) FE-SEM cross sectional image of CNTs/CF<sub>M</sub>.

#### Acknowledgements

The authors would like to express their appreciation and gratitude to the Ministry of Science and Technology (MOST) (Project No. MOST 104-2628-E-029-002-MY2). The authors also would like to thank Prof. Chi-Chang Lin, Department of Chemical and Materials Engineering, Tunghai University in providing the Rama analysis facilities.

#### Authors' contributions

The manuscript draft was interpreted and written by Nhat Huy Luan. Yu-Ting Yang provided technical support. Prof. Chiung-Fen Chang revised the manuscript and supervised the research. All authors read and approved the final manuscript.

#### Funding

This work was supported by Ministry of Science and Technology (MOST) (Project No. MOST 104-2628-E-029-002-MY2).

#### Availability of data and materials

The datasets supporting the conclusions of this article are included within the article and supplementary materials.

#### Declarations

#### Competing interests

The authors declare they have no competing interests.

Received: 27 September 2021 Accepted: 5 January 2022

Published online: 31 January 2022

#### References

- Katheresan V, Kansedo J, Lau SY. Efficiency of various recent wastewater dye removal methods: a review. *J Environ Chem Eng.* 2018;6:4676–97.
- De Gisi S, Lofrano G, Grassi M, Notarnicola M. Characteristics and adsorption capacities of low-cost sorbents for wastewater treatment: a review. *Sustain Mater Technol.* 2016;9:10–40.
- Chen HL, Burns LD. Environmental analysis of textile products. *Cloth Text Res J.* 2006;24:248–61.
- Beakou BH, El Hassani K, Houssaini MA, Belbahloul M, Oukani E, Anouar A. Novel activated carbon from *Manihot esculenta* Crantz for removal of Methylene Blue. *Sustain Environ Res.* 2017;27:215–22.
- Muda K, Aris A, Salim MR, Ibrahim Z. Sequential anaerobic-aerobic phase strategy using microbial granular sludge for textile wastewater treatment.

- Matovic MD, editor. Biomass now sustainable growth and use. Rijeka: InTech Open; 2013. 231–64.
- Fernandes A, Morao A, Magrinho M, Lopes A, Goncalves I. Electrochemical degradation of C.I. Acid Orange 7. *Dyes Pigments*. 2004;61:287–96.
  - Sakalis A, Mpoulmpasakos K, Nickel U, Fytianos K, Voulgaropoulos A. Evaluation of a novel electrochemical pilot plant process for azodyes removal from textile wastewater. *Chem Eng J*. 2005;111:63–70.
  - Peralta-Hernandez JM, de la Rosa-Juarez C, Buzo-Munoz V, Paramo-Vargas J, Canizares-Canizares P, Rodrigo-Rodrigo MA. Synergism between anodic oxidation with diamond anodes and heterogeneous catalytic photolysis for the treatment of pharmaceutical pollutants. *Sustain Environ Res*. 2016;26:70–5.
  - Alaoui A, El Kacemi K, El Ass K, Kitane S, El Bouzidi S. Activity of Pt/MnO<sub>2</sub> electrode in the electrochemical degradation of methylene blue in aqueous solution. *Sep Purif Technol*. 2015;154:281–9.
  - Zhu WL, Michalsky R, Metin O, Lv HF, Guo SJ, Wright CJ, et al. Monodisperse Au nanoparticles for selective electrocatalytic reduction of CO<sub>2</sub> to CO. *J Am Chem Soc*. 2013;135:16833–6.
  - Peterson AA, Norskov JK. Activity descriptors for CO<sub>2</sub> electroreduction to methane on transition-metal catalysts. *J Phys Chem Lett*. 2012;3:251–8.
  - Lee S, Park G, Lee J. Importance of Ag-Cu biphasic boundaries for selective electrochemical reduction of CO<sub>2</sub> to ethanol. *ACS Catal*. 2017;7:8594–604.
  - Ogura K. Electrochemical reduction of carbon dioxide to ethylene: mechanistic approach. *J CO<sub>2</sub> Util*. 2013;1:43–9.
  - Walton SM, He X, Zigler BT, Wooldridge MS. An experimental investigation of the ignition properties of hydrogen and carbon monoxide mixtures for syngas turbine applications. *Proc Combust Inst*. 2007;31:3147–54.
  - Rosen BA, Salehi-Khojin A, Thorson MR, Zhu W, Whipple DT, Kenis PJA, et al. Ionic liquid-mediated selective conversion of CO<sub>2</sub> to CO at low overpotentials. *Science*. 2011;334:643–44.
  - Marselli B, Garcia-Gomez J, Michaud PA, Rodrigo MA, Comninellis C. Electrogeneration of hydroxyl radicals on boron-doped diamond electrodes. *J Electrochem Soc*. 2003;150:D79–83.
  - Ciriaco L, Anjo C, Pacheco MJ, Lopes A, Correia J. Electrochemical degradation of Ibuprofen on Ti/Pt/PbO<sub>2</sub> and Si/BDD electrodes. *Electrochim Acta*. 2009;54:1464–72.
  - Riyanto MM. Electrochemical degradation of methylene blue using carbon composite electrode (C-PVC) in sodium chloride. *IOSR J Appl Chem*. 2015;8:31–40.
  - Duan XC, Xu JT, Wei ZX, Ma JM, Guo SJ, Wang SY, et al. Metal-free carbon materials for CO<sub>2</sub> electrochemical reduction. *Adv Mater*. 2017;29:1701784.
  - Fan L, Zhou YW, Yang WS, Chen GH, Yang FL. Electrochemical degradation of aqueous solution of Amaranth azo dye on ACF under potentiostatic model. *Dyes Pigments*. 2008;76:440–6.
  - Yi FY, Chen SX, Yuan C. Effect of activated carbon fiber anode structure and electrolysis conditions on electrochemical degradation of dye wastewater. *J Hazard Mater*. 2008;157:79–87.
  - Zhao YD, Zhang WD, Chen H, Luo QM. Anodic oxidation of hydrazine at carbon nanotube powder microelectrode and its detection. *Talanta*. 2002;58:529–34.
  - Awad YM, Abuzaid NS. Electrochemical oxidation of phenol using graphite anodes. *Sep Sci Technol*. 1999;34:699–708.
  - Yao ZQ, Wang CG, Wang YX, Lu RJ, Su SS, Qin JJ, et al. Tensile properties of CNTs-grown carbon fiber fabrics prepared using Fe-Co bimetallic catalysts at low temperature. *J Mater Sci*. 2019;54:11841–7.
  - Chen CS, Handoko AD, Wan JH, Ma L, Ren D, Yeo BS. Stable and selective electrochemical reduction of carbon dioxide to ethylene on copper mesocrystals. *Catal Sci Technol*. 2015;5:161–8.
  - Martinez-Huitle CA, Ferro S, De Battisti A. Electrochemical incineration of oxalic acid: role of electrode material. *Electrochim Acta*. 2004;49:4027–34.
  - Iniesta J, Michaud PA, Panizza M, Comninellis C. Electrochemical oxidation of 3-methylpyridine at a boron-doped diamond electrode: application to electroorganic synthesis and wastewater treatment. *Electrochem Commun*. 2001;3:346–51.
  - Gattrell M, Kirk DW. The electrochemical oxidation of aqueous phenol at a glassy carbon electrode. *Can J Chem Eng*. 1990;68:997–1003.
  - Rivas F, Navarrete V, Beltran E, Garcia-Araya JE. Simazine Fenton's oxidation in a continuous reactor. *Appl Catal B Environ*. 2004;48:249–58.
  - Wu WY, Huang ZH, Lim TT. Recent development of mixed metal oxide anodes for electrochemical oxidation of organic pollutants in water. *Appl Catal A Gen*. 2014;480:58–78.
  - Wei HR, Deng SB, Huang Q, Nie Y, Wang B, Huang J, et al. Regenerable granular carbon nanotubes/alumina hybrid adsorbents for diclofenac sodium and carbamazepine removal from aqueous solution. *Water Res*. 2013;47:4139–47.
  - Verma S, Lu X, Ma SC, Masel RI, Kenis PJA. The effect of electrolyte composition on the electroreduction of CO<sub>2</sub> to CO on Ag based gas diffusion electrodes. *Phys Chem Chem Phys*. 2016;18:7075–84.
  - Wu JJ, Yadav RM, Liu MJ, Sharma PP, Tiwary CS, Ma LL, et al. Achieving highly efficient, selective, and stable CO<sub>2</sub> reduction on nitrogen-doped carbon nanotubes. *ACS Nano*. 2015;9:5364–71.
  - Murata A, Hori Y. Product Selectivity affected by cationic species in electrochemical reduction of CO<sub>2</sub> and Co at a Cu electrode. *Bull Chem Soc Jpn*. 1991;64:123–7.
  - Wu JJ, Risalvato FG, Ke FS, Pellechia PJ, Zhou XD. Electrochemical reduction of carbon dioxide I. Effects of the electrolyte on the selectivity and activity with Sn electrode. *J Electrochem Soc*. 2012;159:F353–9.
  - Thorson MR, Siil KI, Kenis PJA. Effect of cations on the electrochemical conversion of CO<sub>2</sub> to CO. *J Electrochem Soc*. 2013;160:F69–74.
  - Srinivasan N, Shiga Y, Atarashi D, Sakai E, Miyauchi M. A PEDOT-coated quantum dot as efficient visible light harvester for photocatalytic hydrogen production. *Appl Catal B Environ*. 2015;179:113–21.
  - Srinivas B, Shubhamangala B, Lalitha K, Reddy PAK, Kumari VD, Subrahmanyam M, et al. Photocatalytic reduction of CO<sub>2</sub> over Cu-TiO<sub>2</sub>/molecular sieve 5A composite. *Photochem Photobiol*. 2011;87:995–1001.
  - Kaneco S, Iiba K, Ohta K, Mizuno T, Saji A. Electrochemical reduction of CO<sub>2</sub> at an Ag electrode in KOH-methanol at low temperature. *Electrochim Acta*. 1998;44:573–8.
  - Azuma M, Hashimoto K, Hiramoto M, Watanabe M, Sakata T. Electrochemical reduction of carbon dioxide on various metal electrodes in low-temperature in aqueous KHCO<sub>3</sub> media. *J Electrochem Soc*. 1990;137:1772–8.

## Publisher's Note

Springer Nature remains neutral with regard to jurisdictional claims in published maps and institutional affiliations.

### Ready to submit your research? Choose BMC and benefit from:

- fast, convenient online submission
- thorough peer review by experienced researchers in your field
- rapid publication on acceptance
- support for research data, including large and complex data types
- gold Open Access which fosters wider collaboration and increased citations
- maximum visibility for your research: over 100M website views per year

At BMC, research is always in progress.

Learn more [biomedcentral.com/submissions](https://biomedcentral.com/submissions)

